ACS APPLIED MATERIALS & INTERFACES

www.acsami.org

Research Article

Ultrawhite $BaSO_4$ Paints and Films for Remarkable Daytime Subambient Radiative Cooling

Xiangyu Li, Joseph Peoples, Peiyan Yao, and Xiulin Ruan*

Cite This: *ACS Appl. Mater. Interfaces* 2021, 13, 21733–21739

Read Online

ACCESS | Metrics & More | Article Recommendations | Supporting Information

ABSTRACT: Radiative cooling is a passive cooling technology that offers great promises to reduce space cooling cost, combat the urban island effect, and alleviate the global warming. To achieve passive daytime radiative cooling, current state-of-the-art solutions often utilize complicated multilayer structures or a reflective metal layer, limiting their applications in many fields. Attempts have been made to achieve passive daytime radiative cooling with single-layer paints, but they often require a thick coating or show partial daytime cooling. In this work, we experimentally demonstrate remarkable full-daytime subambient cooling performance with both $BaSO_4$ nanoparticle films and $BaSO_4$ nanocomposite paints. $BaSO_4$ has a high electron band gap for low solar absorptance and phonon resonance at 9 μm for high sky window emissivity. With an appropriate particle size and a broad particle size distribution, the $BaSO_4$ nanoparticle film reaches an ultrahigh solar reflectance of 97.6% and a high sky window emissivity of 0.96. During field tests, the $BaSO_4$ film stays more than 4.5 °C below ambient temperature or achieves an average cooling power of 117 W/m^2. The $BaSO_4$-acrylic paint is developed with a 60% volume concentration to enhance the reliability in outdoor applications, achieving a solar reflectance of 98.1% and a sky window emissivity of 0.95. Field tests indicate similar cooling performance to the $BaSO_4$ films. Overall, our $BaSO_4$-acrylic paint shows a standard figure of merit of 0.77, which is among the highest of radiative cooling solutions while providing great reliability, convenient paint form, ease of use, and compatibility with the commercial paint fabrication process.

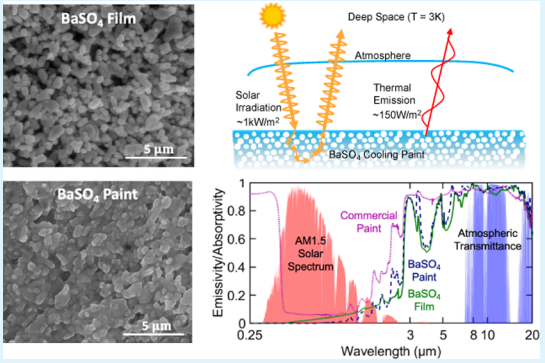

KEYWORDS: *daytime radiative cooling, atmospheric sky window, particle−matrix paint, figure of merit*

INTRODUCTION

Radiative cooling has shown great promises to reduce the cost of space cooling in a variety of cooling applications.[1] Contrary to active cooling, which requires electricity to drive a refrigeration cycle, radiative cooling utilizes the atmospheric transparent window (the "sky window") to emit thermal radiation directly to the deep sky without consuming any energy.[2] Its passive nature has the potential to alleviate the urban island effect by lowering building temperatures and reduce the global warming by reducing the CO_2 emission for cooling applications. With high emissivity in the sky window to outweigh the incoming solar absorption, it is possible for the surface to maintain below ambient even under direct sunlight. Early studies of radiative cooling paints lasted for decades, but full-daytime radiative cooling has not been achieved by these paints.[2−11] Among these, one study showed a 2 °C subambient cooling with a layer of the TiO_2 paint on the aluminum substrate, but the high solar reflectance should primarily come from the metal substrate rather than the paint itself.[9] Many paints were based on TiO_2 with low particle concentration, and the radiative cooling performance was limited by insufficient solar reflection due to the solar absorptance in the ultraviolet (UV) band. For this reason, wide-band-gap materials were explored as fillers[12,13] to eliminate the UV absorption, while their smaller refractive index makes photon scattering weaker. Heat-reflective paints have also been developed, but their solar reflection is still limited below 91% and does not show full-daytime subambient cooling.[11,14] Alternatively, photonic structures and multilayers have recently demonstrated full-daytime subambient cooling capability, which stimulated renewed interest in radiative cooling.[15,16] Other studies explored scalable nonpaint approaches such as dual layers including a metal layer,[17−21] polyethylene aerogel,[22] and delignified wood.[23] However, these approaches are limited in one or more aspects such as the complicated structure, involvement of a metallic layer, and large thickness, preventing them from many applications. In light of this, creating high-performance radiative cooling paints is still a pertinent task. Recently, nonmetal dual-layer designs were proposed consist-

Received: February 3, 2021
Accepted: March 22, 2021
Published: April 15, 2021

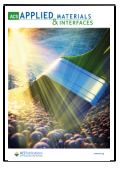

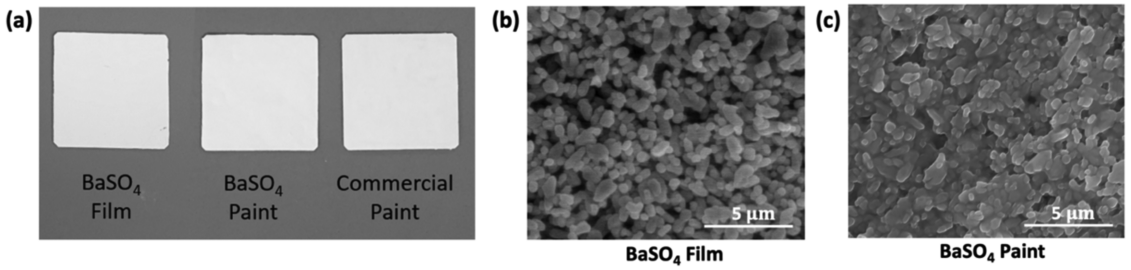

Figure 1. Radiative cooling coatings and SEM images. (a) $BaSO_4$ film sample, $BaSO_4$-acrylic paint sample, and white commercial paint. The $BaSO_4$ film is 150 μm thick on a silicon wafer. The $BaSO_4$ paint and commercial paint are freestanding samples with a thickness of 400 μm. All samples are 5 cm squares. (b) $BaSO_4$ film sample under SEM. (c) $BaSO_4$-acrylic composite paint sample with a 60% filler concentration under SEM. (b, c) Particle size distribution (398 ± 130 nm) was estimated based on the SEM images. Air voids were introduced in both the $BaSO_4$ film and the $BaSO_4$ paint.

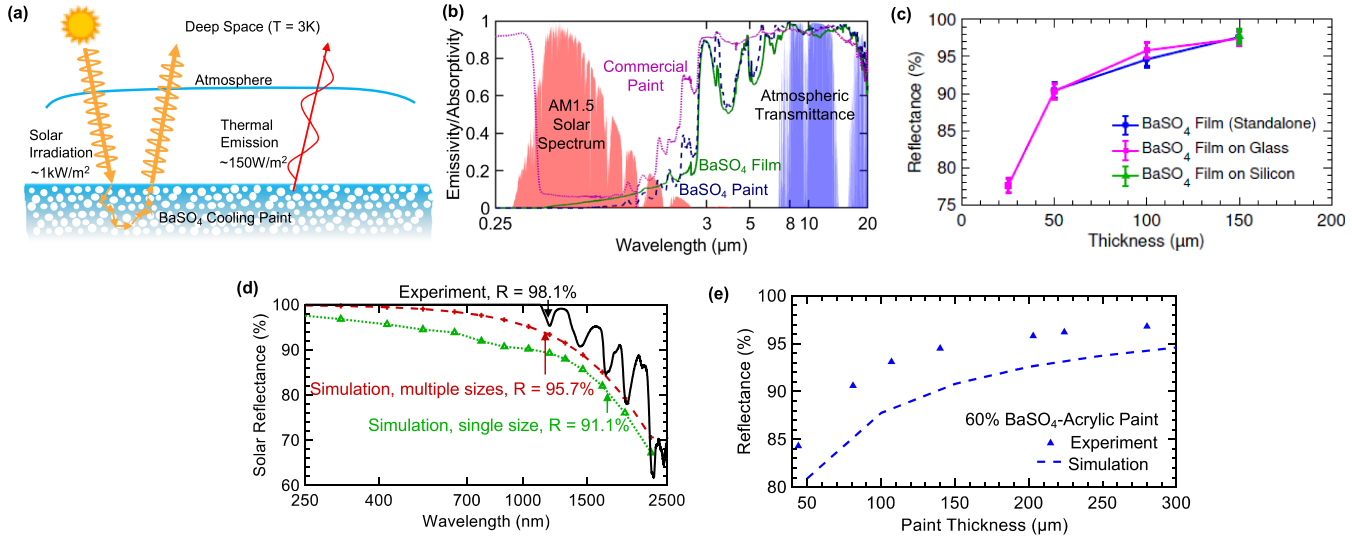

Figure 2. Radiative energy transfer for cooling paints, emissivity characterization results, and Monte Carlo simulation on the solar reflectance. (a) To achieve a high cooling power with passive radiative cooling, both high reflectance in the solar spectrum and high emissivity in the sky window are needed. The solar reflectance is enhanced by filler materials, while the infrared emissivity in the sky window can be contributed by fillers and/or matrix. For particle films, the particles have to both reflect solar light and emit in the sky window. (b) Emissivities of the $BaSO_4$ film and $BaSO_4$ paint were characterized, compared with the commercial white paint (400 μm thick) from 0.25 to 20 μm. Both the particle film and nanocomposite paint showed significant enhancement of solar reflectance while maintaining high sky window emissivity. (c) Solar reflectances of the $BaSO_4$ films with different thicknesses and substrates were measured, demonstrating that the solar reflectance of the $BaSO_4$ film at 150 μm is substrate-independent. (d) Monte Carlo simulation of the $BaSO_4$ paint with a 400 μm thickness demonstrated that both high filler concentration and broad particle size distribution increased the overall solar reflectance. (e) Solar reflectances of the $BaSO_4$-acrylic paint with a 60% particle concentration and different film thicknesses were compared with the Monte Carlo simulation results. The thin paint coatings are supported by PET films.

ing of a top TiO_2 layer for solar reflectance and a bottom layer for thermal emission, which achieved partial daytime cooling without metallic components.[24,25] A compact film of SiO_2 nanoparticles was fabricated as a single-layer coating with partial daytime cooling capability.[26] Paint-like porous polymers were developed with full-daytime cooling.[27] A strategy was proposed to further enhance the solar reflectance in the particle−matrix paint by adopting a broad particle size distribution rather than one single size.[28] Combined with a high filler concentration, the $CaCO_3$-acrylic paint with a layer thickness of 200−400 μm was fabricated and demonstrated full-daytime cooling below ambient temperatures.[29,30] Another study also proposed wide-band-gap nanoparticle paints and high filler concentrations to achieve high radiative cooling performance, but the reported 1 mm coating thickness still posed challenges for potential applications of radiative cooling paints.[31] Considering the existing studies, developing high-performance single-layer coatings that are thin, low cost, easy to apply, and scalable is still a challenging and urgent task to fully utilize radiative cooling in a wide range of applications.

In this work, we experimentally demonstrate full-daytime subambient cooling with $BaSO_4$ nanoparticle films and $BaSO_4$-acrylic paints. We choose $BaSO_4$ due to its high electron band gap for low solar absorptance and phonon resonance at 9 μm for high sky window emissivity. By adopting an appropriate particle size and a broad particle size distribution, we achieve a high solar reflectance of 97.6% and a high sky window emissivity of 0.96 with the $BaSO_4$ nanoparticle film. Field tests indicate surface temperatures more than 4.5 °C below ambient temperatures or an average cooling power of 117 W/m^2, among the highest cooling power reported. To enhance the reliability of the coating, the $BaSO_4$-acrylic paint is developed with a 60% volume concentration. The high filler concentration and the broad particle size distribution are added to overcome the low refractive index of $BaSO_4$, leading to a solar reflectance of 98.1% and a sky window emissivity of 0.95.

https://doi.org/10.1021/acsami.1c02368
ACS Appl. Mater. Interfaces 2021, 13, 21733−21739

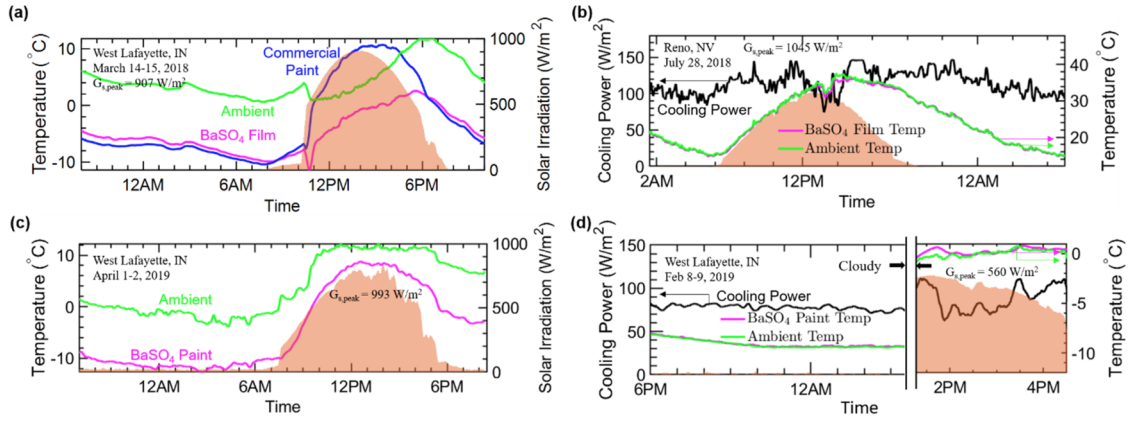

Figure 3. Field test results of the $BaSO_4$ nanoparticle film and $BaSO_4$-acrylic nanocomposite paint. (a) Temperatures of the $BaSO_4$ nanoparticle film and commercial white paint were compared to the ambient temperature for over 24 h. (b) Cooling power of the $BaSO_4$ nanoparticle film was directly characterized by a feedback heater. (c) Temperature of the $BaSO_4$ paint was compared with the ambient temperature. (d) Cooling power of the $BaSO_4$ paint was measured in both daytime and nighttime. The solar irradiation is represented by the orange regions.

During field tests, the $BaSO_4$ paint yields similarly high cooling performance. Our $BaSO_4$-acrylic paint shows a standard figure of merit of 0.77, which is among the highest of radiative cooling solutions while providing great reliability, convenient paint form, ease of use, and compatibility with the commercial paint fabrication process. The results in this paper were included in a provisional patent filed on October 3, 2018 and a nonprovisional international patent application (PCT/US2019/054566) filed on October 3, 2019 and published on April 9, 2020.[32]

RESULTS AND DISCUSSION

Commercial white paints such as the TiO_2-acrylic paint failed to achieve passive full-daytime subambient cooling, which is largely attributed to its high absorption in the UV band (due to the 3.2 eV electron band gap of TiO_2) and near-infrared (NIR) band (due to acrylic absorption). In this work, we fabricated a $BaSO_4$ particle film with a thickness of 150 μm on a silicon wafer (Figure 1a). A commercial white paint (DutchBoy Maxbond UltraWhite Exterior Acrylic Paint) is chosen as a control sample. The scanning electron microscopy (SEM) image of the $BaSO_4$ film in Figure 1b showed air voids in the film. The interfaces between $BaSO_4$ nanoparticles and air voids enhance the photon scattering in the film, thus increasing the overall solar reflectance. To improve the reliability of the coating under long-term outdoor exposure, a commercial paint form as the filler−matrix composite is often preferred. A key challenge to adopt $BaSO_4$ as a filler material in the polymer matrix is its lower refractive index compared to those of other common fillers such as TiO_2. To enable strong scattering in the composite, we adopted a high filler volume concentration of 60%, whereas most commercial paints have much lower concentrations. Additionally, the broad particle size distribution contributes to the solar reflectance.[28] The $BaSO_4$-acrylic nanocomposite paint is shown in Figure 1a with an SEM image in Figure 1c. The addition of acrylic helps bond the fillers and leads to a better reliability. Some air voids were present in the $BaSO_4$ paint, which also increases the solar reflectance. Based on our previous theoretical works, we chose an average particle size of 400 nm, which is beneficial for the overall solar reflectance.[24,28] Furthermore, in the previous work, we identified that a wide particle size distribution (>100 nm) can significantly enhance the overall solar reflectance compared to a uniform particle size distribution.[28] The purchased $BaSO_4$ particles were characterized by SEM to have a particle size distribution of 398 ± 130 nm, which satisfied our needs and met our design guidelines.

To achieve high radiative cooling performance and daytime subambient cooling, the paint requires high reflectance in the solar spectrum (contributed by particles) as well as high emissivity in the sky window (contributed by particles and/or matrix), as illustrated in Figure 2a. Here, we adopted $BaSO_4$ with a high electron band gap of ∼6 eV to reduce the absorption in the UV band. Due to a phonon resonance at 9 μm, which is in the sky window, engineering the particle size can allow a single layer of the $BaSO_4$ particle film to function as both a sky window emitter and a solar reflector. Therefore, the matrix is not needed to achieve daytime subambient cooling. The lack of acrylic matrix also reduces the NIR absorption. The average particle size of $BaSO_4$ was chosen as 400 nm to reflect both visible and NIR ranges of the solar irradiation. A broad particle size distribution was adopted to further enhance the solar reflectance. Detailed theoretical and experimental studies can be found in previous studies.[29] Overall, the $BaSO_4$ film reached a solar reflectance of 97.6% and an emissivity of 0.96 in the sky window (Figure 2b). Its solar reflectance is significantly higher than that of the commercial white paint (400 μm thickness), especially in the UV and NIR ranges. Although heat-reflective commercial paints were introduced in the market, their solar reflectances (around 80−91%) are still much lower than that of the $BaSO_4$ film.[11,14] The solar reflectance of the $BaSO_4$ film is also higher than that of the recently reported $CaCO_3$-acrylic paint.[29] The silicon substrate was intended only as a supporting substrate, neither increasing the solar reflectance nor enhancing the sky window emissivity. To avoid the substrate effect on the cooling performance, we characterized the thickness-dependent solar reflectance with different substrates, shown in Figure 2c. Nighttime cooling performance was also characterized by different substrates in the Supporting Information Note 1 and Figure S1. For the $BaSO_4$ paint, a standalone paint sample of 400 μm reached similar optical properties (98.1% solar reflectance, 0.95 sky window emissivity) with a high filler concentration of 60% and a broad size distribution. A Monte Carlo simulation with the modified Lorentz−Mie theory was run to shine the light on the physics, enabling the high solar reflectance of the paint, and the

https://doi.org/10.1021/acsami.1c02368
ACS Appl. Mater. Interfaces 2021, 13, 21733−21739

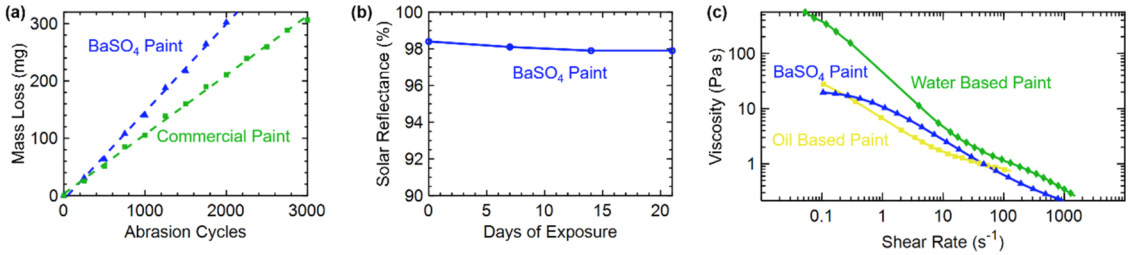

Figure 4. Reliability tests of the $BaSO_4$ paint. (a) Abrasion tests were conducted with the $BaSO_4$ paint and commercial exterior paint according to ASTM D4060.[39] Our $BaSO_4$ paint demonstrated comparable abrasion resistance with commercial exterior paint. (b) We exposed the $BaSO_4$ paint outdoor for a 3-week period. (c) Viscosity of the $BaSO_4$ paint was characterized, which was comparable to those of the oil- and water-based commercial paints.[40]

results are shown in Figure 2d.[28,33] The refractive index of $BaSO_4$ is obtained from the first-principles simulation.[34] With the same filler concentration, the simulation demonstrated a broader particle size distribution, further improving the overall solar reflectance. The simulation slightly underestimated the solar reflectance as it cannot capture the effect of air voids. The $BaSO_4$ paint sample with a 400 μm thickness was to ensure that the characterized emissivity was independent of the substrate. Thinner coatings were fabricated on the transparent poly(ethylene terephthalate) (PET) film using a film applicator to control the wet film thickness. With a low transmittance of the paint films and similar refractive index between the paint and the PET film, the PET substrate had a negligible effect on the solar reflectance. With thinner coating thicknesses of 200, 224, and 280 μm, the solar reflectances reached 95.8, 96.2, and 96.8%, respectively (Figure 2e). Monte Carlo simulation results showed a similar trend to the experimental data, both following the diffusion behavior of the transmission.[26,35] The simulation slightly underestimated the solar reflectance, likely because the air voids introduced in the paint were not captured by the Monte Carlo simulation. Future studies can aim to include such an effect to predict the solar reflectance more accurately.

Onsite field tests were performed to demonstrate the full-daytime subambient cooling of the $BaSO_4$ film. In Figure 3a, the $BaSO_4$ film achieved full subambient daytime cooling with a solar irradiation up to 907 W/m^2 in West Lafayette, IN, on March 14−16, 2018 with a 64% relative humidity at 12 AM and a 50% humidity at 12 PM on March 15, 2018. The temperature of the sample dropped 10.5 °C below the ambient temperature during the nights and maintained 4.5−10 °C below the ambient temperature during daytime, whereas the commercial paint increased 6.8 °C above the ambient temperature at 2−3 PM. A direct measurement of the cooling power in Reno, NV, on July 28, 2018 showed that the cooling power reached an average of 117 W/m^2 over a 24 h period with a 29% relative humidity at 2 AM and a 15% humidity at 12 PM on July 28, 2018, shown in Figure 3b. We observed similar daytime cooling power to nighttime without solar irradiation, both above 110 W/m^2. Thermal emission power increases with a higher surface temperature in the daytime, which compensates the higher solar absorption. Thus, simply reporting the cooling power without considering the surface temperature can be a misleading measure of the cooling performance. In this case, the thermal emissive power of the $BaSO_4$ film reaches 106 W/m^2 at 15 °C. Overall, our $BaSO_4$ film can maintain a constant high cooling power regardless of the solar irradiation. We further demonstrated the cooling performance of the $BaSO_4$ paint with onsite field tests, as shown in Figure 3c,d. The $BaSO_4$ paint remained cooler than ambient for more than 24 h under solar irradiation up to 993 W/m^2 (65% relative humidity at 12 AM, 46% relative humidity at 12 PM on April 2, 2019). The cooling power measurement showed an average cooling power over 80 W/m^2 with the surface temperature as low as −10 °C, equivalent to a cooling power of 113 W/m^2 at 15 °C (77% relative humidity at 12 AM, 57% relative humidity at 2 PM on February 9, 2019). More details are included in the Supporting Information Note 2.

The figure of merit *RC* was used here to fairly access the radiative cooling performance independent of weather conditions, as[29]

$$RC = \epsilon_{sky} - r(1 - R_{solar}) \quad (1)$$

where ϵ_{sky} is the sky window emissivity, R_{solar} is the solar reflectance, and r is the ratio of the solar irradiation over the blackbody emission through the sky window. With a 300 K surface temperature and r as 10, our $BaSO_4$ film and $BaSO_4$ paint reach the standard RCs of 0.72 and 0.77, respectively, which are higher than state-of-the-art radiative cooling solutions as 0.32,[16] 0.53,[18] 0.35,[19] 0.49,[29] and 0.57.[27] The standard figure of merit was proposed to address the concern of the weather effect on the field test results.[29] It is capable of fairly assessing the potential of any radiative cooling solutions under different weather conditions. Accurately predicting the effect of weather conditions on radiative cooling power is still under investigation with other studies.[36−38] We believe that the insights from these field studies combining our figure of merit are essential to predict the actual radiative cooling power and significantly reduce the development cycle of any radiative cooling solutions in the future.

To demonstrate the reliability of our $BaSO_4$ paint, we conducted abrasion test, outdoor weathering, and viscosity characterizations. The abrasion tests were performed according to ASTM D4060 with a Taber Abraser Research Model, and the results are shown in Figure 4a.[39] Two 250 g load abrasive wheels were located on the measured surface. Wheel refacing was done every 500 cycles. By monitoring the mass loss through up to 3,000 cycles, the wear index was characterized as the weight loss (μg) for each cycle. The $BaSO_4$ paint reached a wear index of 150, comparable to the commercial exterior paint with a wear index of 104. The weathering test was conducted by exposing the $BaSO_4$ paint outdoors for 3 weeks (Figure 4b). The solar reflectance remained the same within the experimental uncertainty. The sky window emissivity was measured to be 0.95, at both the beginning and the end of the testing period. Additionally, a running water test is included in Video S1. In Figure 4c, the $BaSO_4$ paint yields similar viscosity

https://doi.org/10.1021/acsami.1c02368
ACS Appl. Mater. Interfaces 2021, 13, 21733−21739

to the commercial paints.[40] Video S1 further demonstrated that the $BaSO_4$ paint was able to be applied with paint brushes and dried similarly to the commercial paints. A detailed cost analysis of the $BaSO_4$ paint is included in Supporting Information Note 3.

EXPERIMENTAL SECTION AND CONCLUSIONS

In this work, we experimentally demonstrate full-daytime radiative cooling with the $BaSO_4$ nanoparticle film and $BaSO_4$-acrylic nanocomposite paint. By adopting an appropriate particle size and a broad particle size distribution, we achieve a high solar reflectance of 97.6% and a high sky window emissivity of 0.96 with the $BaSO_4$ nanoparticle film. Onsite field tests indicate surface temperatures more than 4.5 °C below ambient temperatures or an average cooling power of 117 W/m^2, among the highest cooling power reported. To enhance the reliability of the coating, the $BaSO_4$-acrylic paint is developed with a 60% volume concentration. The high filler concentration and broad particle size distribution help reach a 98.1% solar reflectance and a 0.95 sky window emissivity. During field tests, the $BaSO_4$ paint yields similarly high cooling power while providing great reliability, convenient paint form, ease of use, and compatibility with commercial paints.

$BaSO_4$ Nanoparticle Film and $BaSO_4$-Acrylic Paint Fabrication. A $BaSO_4$ particle film of 150 μm thickness was fabricated on a silicon wafer. 400 nm $BaSO_4$ particles, deionized water, and ethanol were mixed with a mass ratio of 2:1:1 and coated on the substrate until fully dried. The average particle size was chosen as 400 nm to reflect both visible and near-infrared ranges of the solar irradiation. To fabricate the $BaSO_4$-acrylic nanocomposite paint, dimethylformamide and $BaSO_4$ nanoparticles (400 nm diameter, US Research Nanomaterials) were mixed and ultrasonicated for 15 min with a Fisherbrand Model 505 Sonic Dismembrator. The mixture was degassed to remove air bubbles introduced during the ultrasonication process. Acrylic (Elvacite 2028 from Lucite International) was then slowly added and mixed until fully dissolved. The mixture was left fully dried overnight in a mold, resulting in a freestanding sample of 400 μm thickness to eliminate the effect of substrate on the overall coating performance. A series of thinner coatings of the $BaSO_4$ film and paint were also prepared with film applicators (BYK Film Applicator) to study the effect of coating thickness. The dry film thickness was measured with a coordinate measuring machine (Brown&Sharp MicroXcel PFX).

Spectral Emissivity Characterization. The solar reflectance from 250 nm to 2.5 μm was measured with a Perkin Elmer Lambda 950 UV−Vis−NIR spectrometer with an integrating sphere. A certified Spectralon diffuse reflectance standard was used. The overall solar reflectance was estimated based on the AM 1.5 solar spectrum.[41] The uncertainty of the solar reflectance was 0.005 or 0.5% based on the measurement of five samples. The emissivity from 2.5 to 20 μm was characterized by a Nicolet iS50 FTIR with a PIKE Technology integrating sphere. The sky window emissivity was calculated based on the atmospheric transparent window (IR Transmission Spectra, Gemini Observatory, air mass 1.5, and water column 1.0 mm). An uncertainty of 0.02 was estimated based on the mid-IR diffuse reflectance standard from PIKE Technologies.

Field Test. There are two field testing setups made for cooling performance characterization on a building roof, as shown in Figure 5. Similar characterization setups were used in previous studies.[29,32] The setups were created from Styrofoam to reduce thermal conduction and enclosed by a silver mylar to minimize solar absorption of the setups. A pyranometer (Apogee SP-510) was adopted to measure solar irradiation. The temperature measurement setup (Figure 5a) monitored the sample and ambient temperatures with T-type thermocouples. The ambient temperature was monitored by a shaded thermocouple. A low-density polyethylene (LDPE) film functioned as a transparent cover to shield against forced convection. The cooling power characterization setup (Figure 5b) included a feedback heater to characterize the cooling power by heating the samples to the ambient temperature, which minimized heat conduction and convection. A transparent side cover was added to reduce forced convection. The temperature measurement setup provides a direct proof of below-ambient radiative cooling, but it can also be affected by the external wind speed, and the solar absorption of the cavity sidewall, which slightly underestimates the cooling performance of the sample itself. Therefore, in our work, we choose to evaluate the cooling performance mainly from the direct cooling power measurement, which minimizes the parasitic conduction and convection heat transfer.

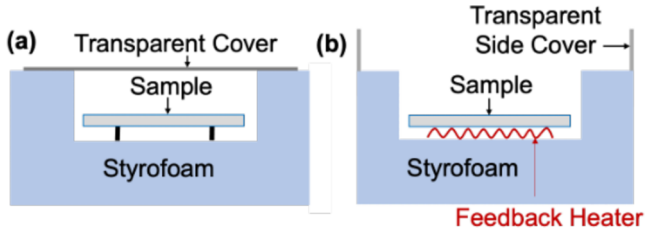

Figure 5. Setups for temperature and cooling power characterization in field tests.[29] (a) Samples were suspended in the Styrofoam cavity to minimize thermal conduction and forced convection. The sample and ambient temperatures were monitored during the temperature measurement. (b) To directly measure the cooling power of the sample, a feedback heater was included to synchronize the sample temperature to the ambient. The cooling power of the sample was obtained by monitoring the heater power consumption.

Monte Carlo Simulation. The Monte Carlo simulations were performed according to the modified Lorentz−Mie theory[28] and a dependent-scattering correction[33] due to high concentrations. Photon packets are initiated above the nanocomposite. The initial weight of the photon packet is unity, traveling normal to the top air−composite interface. As the photon packet propagates through the bottom air−composite interface, we consider it as transmitted. If it travels back above the medium, it is considered reflected. A total of 500,000 photons were used in each simulation, covering 226 wavelengths from 0.25 to 20 μm.

ASSOCIATED CONTENT

Supporting Information

The Supporting Information is available free of charge at https://pubs.acs.org/doi/10.1021/acsami.1c02368.

Substrate dependence of the $BaSO_4$ film samples (Note 1); energy balance model for the cooling power characterization (Note 2); cost analysis of the cooling paint (Note 3); the effect of substrate on the subambient sample temperature of the $BaSO_4$ film (Figure S1); the theoretical cooling power compared with experimental measurements of the $BaSO_4$ film and $BaSO_4$ paint (Figure S2) (PDF)

Brushing, drying, and water running test of the BaSO4 paint (Video S1) (MP4)

AUTHOR INFORMATION

Corresponding Author

Xiulin Ruan − *School of Mechanical Engineering, Purdue University, West Lafayette, Indiana 47907, United States; Birck Nanotechnology Center, Purdue University, West Lafayette, Indiana 47907, United States;* orcid.org/0000-0001-7611-7449; Email: ruan@purdue.edu

Authors

Xiangyu Li − *School of Mechanical Engineering, Purdue University, West Lafayette, Indiana 47907, United States; Birck Nanotechnology Center, Purdue University, West*

Lafayette, Indiana 47907, United States; orcid.org/0000-0003-0116-7307

Joseph Peoples − *School of Mechanical Engineering, Purdue University, West Lafayette, Indiana 47907, United States; Birck Nanotechnology Center, Purdue University, West Lafayette, Indiana 47907, United States;* orcid.org/0000-0002-0495-1394

Peiyan Yao − *School of Mechanical Engineering, Purdue University, West Lafayette, Indiana 47907, United States; Birck Nanotechnology Center, Purdue University, West Lafayette, Indiana 47907, United States*

Complete contact information is available at: https://pubs.acs.org/10.1021/acsami.1c02368

Author Contributions

Conceptualization, X.R.; methodology, X.R., X.L., and J.P.; investigation, X.L., J.P., and P.Y.; writing (original draft) X.L. and X.R.; writing (review and editing), X.R., X.L., J.P., and P.Y.; funding acquisition, X.R.; resources, X.R.; and supervision, X.R. The manuscript was written through contributions of all authors. All authors have given approval to the final version of the manuscript.

Notes

The authors declare the following competing financial interest(s): X.R., X.L., and J.P. are the inventors of an international patent (PCT/US2019/054566) on the basis of the work described here.

■ ACKNOWLEDGMENTS

The authors thank Dr. Mian Wang, Jacob Faulkner, Xuan Li, Nathan Fruehe, Daniel Gallagher, and Professor Zhi Zhou at Purdue University for their help on sample fabrication and characterization. This research was supported by the Cooling Technologies Research Center at Purdue University as well as the Air Force Office of Scientific Research through the Defense University Research Instrumentation Program (Grant No. FA9550-17-1-0368).

■ REFERENCES

(1) Administration, U. S. E. I. Annual Energy Outlook 2018 with Projections to 2050. *J. Phys. A: Math. Theor.* **2018**, *44*, 1−64.
(2) Catalanotti, S.; Cuomo, V.; Piro, G.; Ruggi, D.; Silvestrini, V.; Troise, G. The Radiative Cooling of Selective Surfaces. *Sol. Energy* **1975**, *17*, 83−89.
(3) Granqvist, C. G.; Hjortsberg, A.; Granqvist, G.; Hjortsberg, A. Radiative Cooling to Low Temperatures: General Considerations and Application to Selectively Emitting SiO Films. *J. Appl. Phys.* **1981**, *52*, 4205−4220.
(4) Andretta, A.; Bartoli, B.; Coluzzi, B.; Cuomo, V.; Andretta, A.; Bartoli, B.; Coluzzi, B.; Selective, V. C.; For, S. Selective Surfaces for Natural Cooling Devices. *J. Phys. Colloq.* **1981**, *42*, 423−430.
(5) Lushiku, E. M.; Hjortsberg, A.; Granqvist, C. G. Radiative Cooling with Selectively Infrared-Emitting Ammonia Gas. *J. Appl. Phys.* **1982**, *53*, 5526−5530.
(6) Lushiku, E. M.; Granqvist, C.-G. Radiative Cooling with Selectively Infrared-Emitting Gases. *Appl. Opt.* **1984**, *23*, 1835−1843.
(7) Diatezua, D. M.; Thiry, P. A.; Dereux, A.; Caudano, R. Silicon Oxynitride Multilayers as Spectrally Selective Material for Passive Radiative Cooling Applications. *Sol. Energy Mater. Sol. Cells* **1996**, *40*, 253−259.
(8) Gentle, A. R.; Smith, G. B. Radiative Heat Pumping from the Earth Using Surface Phonon Resonant Nanoparticles. *Nano Lett.* **2010**, *10*, 373−379.
(9) Harrison, A. W. Radiative Cooling of TiO2 White Paint. *Sol. Energy* **1978**, *20*, 185−188.
(10) Orel, B.; Gunde, M. K.; Krainer, A. Radiative Cooling Efficiency of White Pigmented Paints. *Sol. Energy* **1993**, *50*, 477−482.
(11) Pockett, J. Heat Reflecting Paints and a Review of Their Advertising Material. In *Chemeca 2010: Engineering at the Edge*; Hilton Adelaide: South Australia, 2010; pp 1−13.
(12) Nilsson, T. M. J.; Niklasson, G. A. Radiative Cooling during the Day: Simulations and Experiments on Pigmented Polyethylene Cover Foils. *Sol. Energy Mater. Sol. Cells* **1995**, *37*, 93−118.
(13) Grum, F.; Luckey, G. W. Optical Sphere Paint and a Working Standard of Reflectance. *Appl. Opt.* **1968**, *7*, 2289−2294.
(14) Berdahl, P.; Bretz, S. E. Preliminary Survey of the Solar Reflectance of Cool Roofing Materials. *Energy Build.* **1997**, *25*, 149−158.
(15) Rephaeli, E.; Raman, A.; Fan, S. Ultrabroadband Photonic Structures to Achieve High-Performance Daytime Radiative Cooling. *Nano Lett.* **2013**, *13*, 1457−1461.
(16) Raman, A. P.; Anoma, M. A.; Zhu, L.; Rephaeli, E.; Fan, S. Passive Radiative Cooling below Ambient Air Temperature under Direct Sunlight. *Nature* **2014**, *515*, 540−544.
(17) Gentle, A. R.; Smith, G. B. A Subambient Open Roof Surface under the Mid-Summer Sun. *Adv. Sci.* **2015**, *2*, No. 1500119.
(18) Zhai, Y.; Ma, Y.; David, S. N.; Zhao, D.; Lou, R.; Tan, G.; Yang, R.; Yin, X. Scalable-Manufactured Randomized Glass-Polymer Hybrid Metamaterial for Daytime Radiative Cooling. *Science* **2017**, *7899*, 1062−1066.
(19) Kou, J.; Jurado, Z.; Chen, Z.; Fan, S.; Minnich, A. J. Daytime Radiative Cooling Using Near-Black Infrared Emitters. *ACS Photonics* **2017**, *4*, 626−630.
(20) Yang, P.; Chen, C.; Zhang, Z. M. A Dual-Layer Structure with Record-High Solar Reflectance for Daytime Radiative Cooling. *Sol. Energy* **2018**, *169*, 316−324.
(21) Liu, C.; Fan, J.; Bao, H. Hydrophilic Radiative Cooler for Direct Water Condensation in Humid Weather. *Sol. Energy Mater. Sol. Cells* **2020**, *216*, No. 110700.
(22) Leroy, A.; Bhatia, B.; Kelsall, C. C.; Castillejo-Cuberos, A.; Di Capua, H. M.; Zhao, L.; Zhang, L.; Guzman, A. M.; Wang, E. N. High-Performance Subambient Radiative Cooling Enabled by Optically Selective and Thermally Insulating Polyethylene Aerogel. *Sci. Adv.* **2019**, *5*, No. eaat9480.
(23) Li, T.; Zhai, Y.; He, S.; Gan, W.; Wei, Z.; Heidarinejad, M.; Dalgo, D.; Mi, R.; Zhao, X.; Song, J.; Dai, J.; Chen, C.; Aili, A.; Vellore, A.; Martini, A.; Yang, R.; Srebric, J.; Yin, X.; Hu, L. A Radiative Cooling Structural Material. *Science* **2019**, *364*, 760−763.
(24) Huang, Z.; Ruan, X. Nanoparticle Embedded Double-Layer Coating for Daytime Radiative Cooling. *Int. J. Heat Mass Transfer* **2017**, *104*, 890−896.
(25) Bao, H.; Yan, C.; Wang, B.; Fang, X.; Zhao, C. Y.; Ruan, X. Double-Layer Nanoparticle-Based Coatings for Efficient Terrestrial Radiative Cooling. *Sol. Energy Mater. Sol. Cells* **2017**, *168*, 78−84.
(26) Atiganyanun, S.; Plumley, J.; Han, S. J.; Hsu, K.; Cytrynbaum, J.; Peng, T. L.; Han, S. M.; Han, S. E. Effective Radiative Cooling by Paint-Format Microsphere-Based Photonic Random Media. *ACS Photonics* **2018**, *5*, 1181−1187.
(27) Mandal, J.; Fu, Y.; Overvig, A.; Jia, M.; Sun, K.; Shi, N.; Zhou, H.; Xiao, X.; Yu, N.; Yang, Y. Hierarchically Porous Polymer Coatings for Highly Efficient Passive Daytime Radiative Cooling. *Science* **2018**, *362*, 315−319.
(28) Peoples, J.; Li, X.; Lv, Y.; Qiu, J.; Huang, Z.; Ruan, X. A Strategy of Hierarchical Particle Sizes in Nanoparticle Composite for Enhancing Solar Reflection. *Int. J. Heat Mass Transfer* **2019**, *131*, 487−494.
(29) Li, X.; Peoples, J.; Huang, Z.; Zhao, Z.; Qiu, J.; Ruan, X. Full Daytime Sub-Ambient Radiative Cooling in Commercial-like Paints with High Figure of Merit. *Cell Rep. Phys. Sci.* **2020**, *1*, No. 100221.
(30) Li, X. *Engineering Nanocomposites and Interfaces for Conduction and Radiation Thermal Management*; Purdue University Graduate School, 2019.

(31) Mandal, J.; Yang, Y.; Yu, N.; Raman, A. P. Paints as a Scalable and Effective Radiative Cooling Technology for Buildings. *Joule* **2020**, *4*, 1350−1356.
(32) Ruan, X.; Li, X.; Huang, Z.; Peoples, J. A. Metal-Free Solar-Reflective Infrared-Emissive Paints and Methods of Producing the Same, PCT/US2019/054566, 2019. https://patentscope.wipo.int/search/en/detail.jsf.
(33) Kaviany, M. *Principles of Heat Transfer in Porous Media*; Springer: New York, 2012.
(34) Tong, Z.; Peoples, J.; Li, X.; Yang, X.; Bao, H.; Ruan, X. *Atomistic Metrics of BaSO4 as an Ultra-Efficient Radiative Cooling Material: A First-Principles Prediction*. 2021, arXiv:2101.0505. arXiv.org e-Print archive. http://arxiv.org/abs/2101.05053.
(35) Ishimaru, A. *Wave Propagation and Scattering in Random Media*; Academic Press: New York, 1978.
(36) Harrison, A. W. Effect of Atmospheric Humidity on Radiation Cooling. *Sol. Energy* **1981**, *26*, 243−247.
(37) Liu, C.; Wu, Y.; Wang, B.; Zhao, C. Y.; Bao, H. Effect of Atmospheric Water Vapor on Radiative Cooling Performance of Different Surfaces. *Sol. Energy* **2019**, *183*, 218−225.
(38) Feng, J.; Gao, K.; Santamouris, M.; Shah, K. W.; Ranzi, G. Dynamic Impact of Climate on the Performance of Daytime Radiative Cooling Materials. *Sol. Energy Mater. Sol. Cells* **2020**, *208*, No. 110426.
(39) ASTM Standard D4060. *Standard Test Method for Abrasion Resistance of Organic Coatings by the Taber Abraser*; ASTM International, 2010.
(40) Whittingstall, P. Paint Evaluation Using Rheology, A Instruments Publication Rh059, 2011. http://www.tainstruments.com/library_download.aspx.
(41) ASTM Standard G173-03. *Standard Tables for Reference Solar Spectral Irradiances: Direct Normal and Hemispherical on 37° Tilted Surface*; ASTM International: West Conshohocken, PA, 2020.

https://doi.org/10.1021/acsami.1c02368
ACS Appl. Mater. Interfaces 2021, 13, 21733−21739